

## Capture cross section measurements of $^{186,187,188}\text{Os}$ at n\_TOF: the resolved resonance region

K. Fujii<sup>1,a</sup>, M. Mosconi<sup>2</sup>, P.M. Milazzo<sup>1</sup>, C. Domingo-Pardo<sup>2,3</sup>, F. Käppeler<sup>2</sup>, A. Mengoni<sup>4,5</sup>, U. Abbondanno<sup>1</sup>, G. Aerts<sup>6</sup>, H. Álvarez<sup>7</sup>, F. Álvarez-Velarde<sup>8</sup>, S. Andriamonje<sup>6</sup>, J. Andrzejewski<sup>9</sup>, P. Assimakopoulos<sup>7,10</sup>, L. Audouin<sup>11</sup>, G. Badurek<sup>12</sup>, P. Baumann<sup>13</sup>, F. Bečvář<sup>14</sup>, E. Berthoumieux<sup>6</sup>, F. Calviño<sup>15</sup>, M. Calviani<sup>16,17</sup>, D. Cano-Ott<sup>8</sup>, R. Capote<sup>4,18</sup>, C. Carrapiço<sup>6,19</sup>, P. Cennini<sup>5</sup>, V. Chepel<sup>20</sup>, E. Chiaveri<sup>5</sup>, N. Colonna<sup>21</sup>, G. Cortes<sup>22</sup>, A. Couture<sup>23</sup>, J. Cox<sup>23</sup>, M. Dahlfors<sup>5</sup>, S. David<sup>11</sup>, I. Dillmann<sup>2</sup>, W. Dridi<sup>6</sup>, I. Duran<sup>7</sup>, C. Eleftheriadis<sup>24</sup>, M. Embid-Segura<sup>8</sup>, L. Ferrant<sup>7,11</sup>, A. Ferrari<sup>5</sup>, R. Ferreira-Marques<sup>20</sup>, W. Furman<sup>25</sup>, I. Gonçalves<sup>20</sup>, E. González-Romero<sup>8</sup>, F. Gramegna<sup>16</sup>, C. Guerrero<sup>8</sup>, F. Gunsing<sup>6</sup>, B. Haas<sup>26</sup>, R. Haight<sup>27</sup>, M. Heil<sup>2</sup>, A. Herrera-Martinez<sup>5</sup>, M. Igashira<sup>28</sup>, E. Jericha<sup>12</sup>, Y. Kadi<sup>5</sup>, D. Karadimos<sup>10</sup>, D. Karamanis<sup>10</sup>, M. Kerveno<sup>13</sup>, P. Koehler<sup>29</sup>, E. Kossionides<sup>30</sup>, M. Krčička<sup>14</sup>, C. Lampoudis<sup>6,24</sup>, H. Leeb<sup>12</sup>, A. Lindote<sup>20</sup>, I. Lopes<sup>20</sup>, M. Lozano<sup>18</sup>, S. Lukic<sup>13</sup>, J. Marganec<sup>9</sup>, S. Marrone<sup>21</sup>, T. Martínez<sup>8</sup>, C. Massimi<sup>31</sup>, P. Mastinu<sup>16</sup>, C. Moreau<sup>1</sup>, F. Neves<sup>20</sup>, H. Oberhummer<sup>12</sup>, S. O'Brien<sup>23</sup>, J. Pancin<sup>6</sup>, C. Papachristodoulou<sup>10</sup>, C. Papadopoulos<sup>32</sup>, C. Paradela<sup>7</sup>, N. Patronis<sup>10</sup>, A. Pavlik<sup>33</sup>, P. Pavlopoulos<sup>34</sup>, L. Perrot<sup>6</sup>, M.T. Pigni<sup>12</sup>, R. Plag<sup>2</sup>, A. Plompen<sup>35</sup>, A. Plukis<sup>6</sup>, A. Poch<sup>22</sup>, J. Praena<sup>16</sup>, C. Pretel<sup>22</sup>, J. Quesada<sup>18</sup>, T. Rauscher<sup>36</sup>, R. Reifarth<sup>27</sup>, C. Rubbia<sup>37</sup>, G. Rudolf<sup>13</sup>, P. Rullhusen<sup>35</sup>, J. Salgado<sup>19</sup>, C. Santos<sup>19</sup>, L. Sarchiapone<sup>5</sup>, I. Savvidis<sup>24</sup>, C. Stephan<sup>11</sup>, G. Tagliente<sup>21</sup>, J.L. Tain<sup>3</sup>, L. Tassan-Got<sup>11</sup>, L. Tavora<sup>19</sup>, R. Terlizzi<sup>21</sup>, G. Vannini<sup>31</sup>, P. Vaz<sup>19</sup>, A. Ventura<sup>38</sup>, D. Villamarin<sup>8</sup>, M.C. Vicente<sup>8</sup>, V. Vlachoudis<sup>5</sup>, R. Vlastou<sup>32</sup>, F. Voss<sup>2</sup>, S. Walter<sup>2</sup>, M. Wiescher<sup>23</sup>, and K. Wisshak<sup>2</sup>

The n\_TOF Collaboration ([www.cern.ch/ntof](http://www.cern.ch/ntof))

<sup>1</sup>Istituto Nazionale di Fisica Nucleare, Trieste, Italy – <sup>2</sup>Forschungszentrum Karlsruhe GmbH (FZK), Institut für Kernphysik, Germany – <sup>3</sup>Instituto de Física Corpuscular, CSIC-Universidad de Valencia, Spain – <sup>4</sup>International Atomic Energy Agency (IAEA), Nuclear Data Section, Vienna, Austria – <sup>5</sup>CERN, Geneva, Switzerland – <sup>6</sup>CEA/Saclay-DSM/DAPNIA, Gif-sur-Yvette, France – <sup>7</sup>Universidade de Santiago de Compostela, Spain – <sup>8</sup>Centro de Investigaciones Energeticas Medioambientales y Tecnológicas, Madrid, Spain – <sup>9</sup>University of Lodz, Lodz, Poland – <sup>10</sup>University of Ioannina, Greece – <sup>11</sup>Centre National de la Recherche Scientifique/IN2P3-IPN, Orsay, France – <sup>12</sup>Atominstytut der Österreichischen Universitäten, Technische Universität Wien, Austria – <sup>13</sup>Centre National de la Recherche Scientifique/IN2P3-IReS, Strasbourg, France – <sup>14</sup>Charles University, Prague, Czech Republic – <sup>15</sup>Universidad Politecnica de Madrid, Spain – <sup>16</sup>Istituto Nazionale di Fisica Nucleare, Laboratori Nazionali di Legnaro, Italy – <sup>17</sup>Dipartimento di Fisica, Università di Padova, Italy – <sup>18</sup>Universidad de Sevilla, Spain – <sup>19</sup>Instituto Tecnológico e Nuclear (ITN), Lisbon, Portugal – <sup>20</sup>LIP-Coimbra & Departamento de Física da Universidade de Coimbra, Portugal – <sup>21</sup>Istituto Nazionale di Fisica Nucleare, Bari, Italy – <sup>22</sup>Universitat Politècnica de Catalunya, Barcelona, Spain – <sup>23</sup>University of Notre Dame, Notre Dame, USA – <sup>24</sup>Aristotle University of Thessaloniki, Greece – <sup>25</sup>Joint Institute for Nuclear Research, Frank Laboratory of Neutron Physics, Dubna, Russia – <sup>26</sup>Centre National de la Recherche Scientifique/IN2P3-CENBG, Bordeaux, France – <sup>27</sup>Los Alamos National Laboratory, New Mexico, USA – <sup>28</sup>Tokyo Institute of Technology, Tokyo, Japan – <sup>29</sup>Oak Ridge National Laboratory, Physics Division, Oak Ridge, USA – <sup>30</sup>NCSR, Athens, Greece – <sup>31</sup>Dipartimento di Fisica, Università di Bologna, and Sezione INFN di Bologna, Italy – <sup>32</sup>National Technical University of Athens, Greece – <sup>33</sup>Institut für Isotopenforschung und Kernphysik, Universität Wien, Austria – <sup>34</sup>Pôle Universitaire Léonard de Vinci, Paris-La Défense, France – <sup>35</sup>CEC-JRC-IRMM, Geel, Belgium – <sup>36</sup>Department of Physics-University of Basel, Switzerland – <sup>37</sup>Università degli Studi Pavia, Pavia, Italy – <sup>38</sup>ENEA, Bologna, Italy

**Abstract.** The neutron capture cross sections of  $^{186,187,188}\text{Os}$  have been measured at the CERN neutron time-of-flight facility, n\_TOF, in the neutron energy range from 1 eV up to 1 MeV. In this contribution, we report the results of the analysis of the resolved resonance region (RRR). Resonance parameters have been extracted from a full R-matrix fit of the capture yields with the SAMMY code. A statistical analysis has been performed and the related average resonance parameters are derived. This information is crucial for a complete understanding and modeling in terms of the Hauser-Feshbach statistical model of the capture and inelastic reaction channels, required for the evaluation of the stellar reaction rates of these isotopes. Maxwellian average cross sections for the range of temperatures relevant for s-process nucleosynthesis have been derived from the combined information of the experimental data in the resolved and unresolved resonance regions. A brief account of the implications of this analysis in the estimation of the s-process component of the  $^{187}\text{Os}$  abundance and the related impact on the estimates of the time-duration of the galactic nucleosynthesis through the Re/Os clock is given.

### 1 Introduction

The nucleosynthesis of Os and Re (in the mass region  $A \approx 190$ ) presents interesting aspects which have been object

of considerable attention in the past as well as at present. While both  $^{186}\text{Os}$  and  $^{187}\text{Os}$  isotopes are synthesized only by the s-process (they are “shielded” against r-process production by two stable isobars), an important fraction of the observed abundance of  $^{187}\text{Os}$  is due to the slow  $\beta$ -decay of  $^{187}\text{Re}$

<sup>a</sup> Presenting author, e-mail: [kfujii@ts.infn.it](mailto:kfujii@ts.infn.it)

(half-life: 41.2 Gyr). Clayton [1], proposed to use this situation to estimate the time-duration of the galactic nucleosynthesis, and hence, the age of the Universe (the Re/Os clock).

For the analysis of the Re/Os clock, essential nuclear data are the accurate neutron capture cross sections of the  $^{186}\text{Os}$  and  $^{187}\text{Os}$  isotopes, and the  $\beta$ -decay rate of  $^{187}\text{Re}$  under stellar conditions. The latter information has been firmly established by a measurement of the  $^{187}\text{Re}$  half-life for fully-stripped atoms [2]. In the present work, we will address the question of the neutron capture rates. In fact, in the classical s-process picture, the abundance ratio of this isotopic pair is directly related to the ratio of their neutron capture cross sections.

Stellar neutron capture rates are needed namely, cross section averaged over a Maxwellian distribution of neutron energies (MACS), for nuclei in their ground state, as well as in low-lying excited states. In order to derive the stellar MACS, theoretical calculations based on the Hauser-Feshbach statistical model theory (HFSM) are currently performed. It is well known that only with a sound experimental determination of the parameters used in HFSM calculations, acceptable prediction of the required accuracy can be obtained. Among these, average resonance parameters such as mean level spacings  $\langle D \rangle$ , average radiative widths  $\langle \Gamma_\gamma \rangle$  and neutron strength functions  $S$  are the most important quantities which can (and should) be determined experimentally from neutron capture cross section measurements to establish a reliable parametrization of the HFSM calculation.

Additional constraints on the HFSM calculations can be established from a measurement of the inelastic scattering cross section. This quantity provides information on the neutron transmission functions for excited nuclear levels. In fact, this additional study has been performed in a measurement of the inelastic cross section of  $^{187}\text{Os}$ , populating the first excited state in this nucleus [3].

In this contribution we report on the RRR analysis of the  $^{186,187,188}\text{Os}$  neutron capture cross section measurements, aiming at improving the nuclear data requirements for the Re/Os clock.

## 2 Capture measurements at the n\_TOF facility

### 2.1 The n\_TOF facility

The measurements have been performed using the n\_TOF pulsed neutron beam. At n\_TOF, neutrons are generated by spallation reactions induced by the 20 GeV protons beam of the CERN PS accelerator complex impinging on a massive lead target [4]. The low repetition frequency of the proton beam driver, the extremely high instantaneous neutron flux, the low background conditions in the experimental area, together with improvements of the neutron sensitivity of the capture detectors make this facility unique for neutron induced reaction cross section measurements, with much improved accuracy [5]. The generated neutrons are slowed down in the lead spallation target and moderated in the surrounding cooling water. An evacuated flight path with collimators at 135 and 175 m leads to the measuring station at a distance of 185.2 m from the spallation target. The available neutron energy in the experimental area runs from 1 eV up to 250 MeV

with a nearly 1/E isoethargic fluence up to 1 MeV. The neutron beam line extends for additional 12 m beyond the experimental area to minimize the background from back-scattered neutrons. Background due to fast charged particles is suppressed by a 1.5 T sweeping magnet, heavy concrete walls, and a 3.5 m thick iron shielding [5].

### 2.2 Experimental setup

The characteristics of the Os samples used in the present measurements are listed in table 1. Enriched samples were used, 14.9 mm in diameter, encapsulated in a thin aluminum can. Additional samples of C, Pb, and Au were used for flux and background measurements.

The measurement is based on the detection of the  $\gamma$ -rays emitted in the de-excitation cascade following a neutron capture event. Two  $\gamma$ -ray detectors, consisting of  $\text{C}_6\text{D}_6$  liquid scintillator, with minimized neutron sensitivity [6], were placed perpendicular to the neutron beam at a distance of about 3 cm from the beam axis. The background due to in-beam  $\gamma$ -rays [5] is strongly reduced by placing the detectors 9.2 cm upstream of the sample position. The light output of the detectors was periodically calibrated by means of radioactive  $^{137}\text{Cs}$ ,  $^{60}\text{Co}$   $\gamma$ -ray sources and a composite source of the  $\alpha$ -emitter  $^{238}\text{Pu}$  and C, giving a 6.13 MeV  $\gamma$ -ray through the  $^{13}\text{C}(\alpha, n)^{16}\text{O}$  reaction. The calibrated neutron time of flight was used to determine the neutron energy.

The relative neutron flux was measured upstream of the capture samples with a low mass flux monitor consisting of a Mylar foil 1.5  $\mu\text{m}$  in thickness with a layer of 200  $\mu\text{g}/\text{cm}^2$  of  $^6\text{Li}$  surrounded by four Silicon detectors outside the neutron beam, measuring the charged particles of the  $^6\text{Li}(n, \alpha)^3\text{H}$  reaction [7]. The stability of the experimental set-up and the neutron beam was periodically checked.

### 2.3 Data analysis

The detector signals were recorded with fast flash ADC using the standard n\_TOF data acquisition system [8].

The Pulse Height Weighting Function Technique (PHWT) [9], by suitably modifying via software the response function of the detector, allows to proceed in the data analysis in an independent way from the  $\gamma$ -ray spectrum of the prompt capture  $\gamma$ -ray cascade. The weighting functions for the various samples have been calculated on the basis of Monte Carlo simulations of the detector response [10,11]. The cross sections were obtained after a complete evaluation of the background and normalization, i.e. a carbon sample for the effect of scattered neutrons, a lead sample for the

**Table 1.** Characteristics of samples.

Sample	Mass (g)	Thickness (atoms/b)	Enrichment (%)
$^{186}\text{Os}$	1.9999	$3.714 \times 10^{-3}$	79.48
$^{187}\text{Os}$	1.9212	$3.549 \times 10^{-3}$	70.43
$^{188}\text{Os}$	1.9967	$3.669 \times 10^{-3}$	94.99

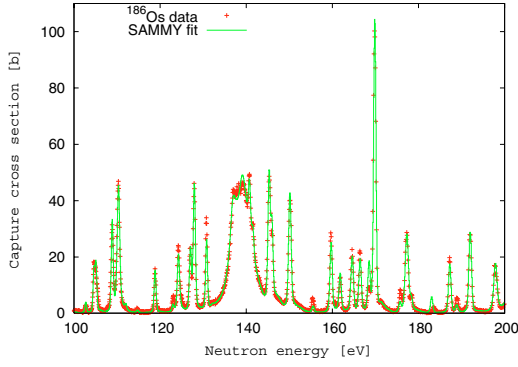


Fig. 1. Resonance fit for the  $^{186}\text{Os}$  sample.

scattering of in-beam  $\gamma$ -rays, a gold sample for the neutron flux normalization and an empty position for obtaining the ambient background component. The cross section and the resonance parameters were extracted from the analysis of the background-subtracted yields.

The analysis of the resonance-dominated yields were done with the R-matrix code SAMMY[12] using the Reich-Moore formalism and including corrections for self-shielding and self-absorption. In the largest majority of cases, the neutron widths ( $\Gamma_n$ ) from transmission experiments [13, 14] have been adopted and the radiative widths ( $\Gamma_\gamma$ ) and the neutron energy ( $E$ ) obtained from the R-matrix fit. The resonance parameters are extracted for  $^{186}\text{Os}$  up to 3.4 keV, for  $^{187}\text{Os}$  up to 2.0 keV, and for  $^{188}\text{Os}$  up to 5.0 keV.

The  $^{186}\text{Os}$  and  $^{188}\text{Os}$  levels belong to a single spin population for s-wave ( $J = 1/2$ ). In the case of  $^{187}\text{Os}$ , the ground-state spin is  $I = 1/2$ , therefore two values of the total angular momentum,  $J = 0$  and  $J = 1$ , are possible for s-wave.

An illustrative example of the SAMMY fit of  $^{186}\text{Os}$  data is shown in figure 1. All the observed resonances can be confidently assumed to be s-wave, an assumption verified by means of statistical methods.

### 3 Statistical analysis and average parameters

The required parameters for statistical model calculations,  $\langle D_0 \rangle$ ,  $\langle \Gamma_\gamma \rangle$  and  $S_0$  are estimated with the parameter sets obtained from the analysis of RRR. Several methods have been used for these estimates as described here below.

Staircase plots, cumulative sums of numbers of resonances as a function of the neutron energy are shown in figure 2. Straight-line fits to the data are from a least square analysis up to the neutron highest energy. From the inverse slope, s-wave average level spacings  $\langle D_0 \rangle$  are obtained and shown in table 2.  $\langle D_0 \rangle$  can also be obtained using a maximum-likelihood estimate assuming a Wigner distribution for the level spacing. The values obtained in this way are completely consistent with those from the straight-line fit of the cumulative number of levels. Histograms of the nearest-neighbor spacing for each spectrum in comparisons with theoretical distribution models are shown in figure 3. As expected, the Wigner

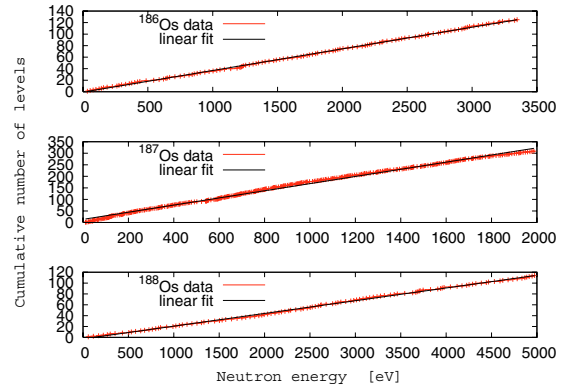


Fig. 2. The cumulative number of levels.

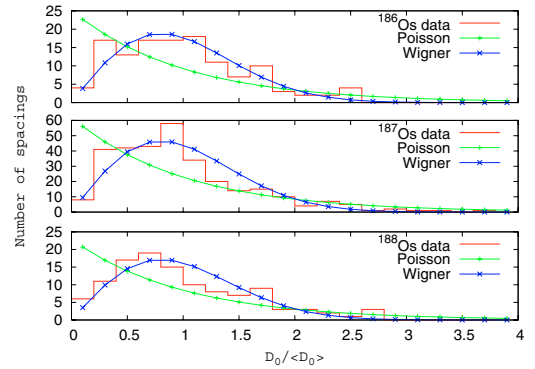


Fig. 3. Nearest-neighbor spacing histograms.

distribution,

$$P_{\text{Wigner}}(s) = \frac{\pi s}{2} e^{-\frac{\pi s^2}{4}} \quad (1)$$

with  $s \equiv D/\langle D \rangle$ , gives the best representation of the experimental data. In comparison to previous experimental data [15], the estimated average level spacings of  $^{186}\text{Os}$  and  $^{188}\text{Os}$  are lower.

The evaluated averaged radiative widths  $\langle \Gamma_\gamma \rangle$  with their uncertainties (statistical) are shown in table 2.

The neutron width distribution is only slightly affected by missing or spurious levels. As well known, a Gaussian distribution of reduced neutron width ( $\Gamma_n^0 = \Gamma_n/\sqrt{E}$ ) amplitudes leads to the Porter-Thomas (P-T) distribution. In estimating the average level widths, we have assumed that they obey P-T distribution and the larger widths are accurately measured. Moreover, the missing level estimator [16] is utilized to evaluate  $\langle g\Gamma_n^0 \rangle$ , here  $g = (2J + 1)/(2(2I + 1))$  is the statistical weight factor. This method is used to derive various moments of the distribution of the reduced neutron width. Estimated  $\langle g\Gamma_n^0 \rangle$  are also shown in table 2.

Table 2. Summary of average resonance parameters (preliminary).

Sample	$\langle D_0 \rangle$ (eV)	$\langle \Gamma_\gamma \rangle$ (meV)	$\langle g\Gamma_n^0 \rangle$ (meV)	$S_0 (\times 10^{-4})$
$^{186}\text{Os}$	$26.6 \pm 0.2$	$45.5 \pm 1.7$	$6.5 \pm 0.8$	$2.45 \pm 0.33$
$^{187}\text{Os}$	$6.5 \pm 0.1$	$64.9 \pm 2.3$	$2.7 \pm 0.2$	$4.11 \pm 0.35$
$^{188}\text{Os}$	$42.7 \pm 0.5$	$51.1 \pm 1.4$	$11.1 \pm 1.6$	$2.60 \pm 0.37$

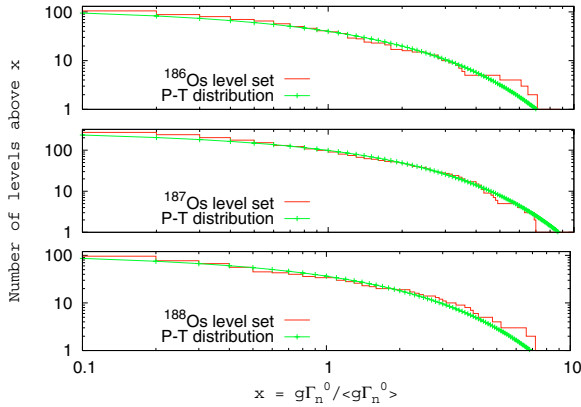


**Fig. 4.** Histograms of reduced neutron widths and P-T distribution.

The integrated P-T distribution for a single-level population can be written,

$$N(x) = N_0 \left[ 1 - \operatorname{erf} \sqrt{x/2} \right], \quad x \equiv g\Gamma_n^0 / \langle g\Gamma_n^0 \rangle. \quad (2)$$

Here  $N_0$  represents the number of resonances. The our data sets of  $g\Gamma_n^0$  with P-T distribution are compared in figure 4.

Finally, the neutron strength function for s-wave  $S_0$  is defined as,

$$S_0 = \frac{\langle g\Gamma_n^0 \rangle}{\langle D_0 \rangle} \left( 1 \pm \sqrt{\frac{2.27}{N_0}} \right). \quad (3)$$

The uncertainty in  $S_0$  is derived assuming a P-T distribution for the reduced neutron widths and a Wigner distribution for the level spacing, respectively. The values thus obtained of  $^{186}\text{Os}$  and  $^{188}\text{Os}$  are in agreement with the values reported by Mughabghab [13].

#### 4 Implication on Re/Os clock

The results of the neutron capture cross sections measured at n\_TOF including the unresolved resonance region (URR) [17] can be used to analyze their impact on the estimation of the age from the Re/Os clock. The capture cross section ratio of the laboratory MACS at 30 keV for  $^{186}\text{Os}$  and  $^{187}\text{Os}$  reported in ref. [17] is  $R_\sigma = 0.42 \pm 0.02$ . This ratio needs to be corrected for the stellar enhancement factor, SEF, arising from the thermal distribution of the target states in a stellar environment. The SEFs for the  $^{186}\text{Os}$  and  $^{187}\text{Os}$  capture cross section have been calculated using HFSM theory on the basis of the statistical parameters determined here for these isotopes. The result implies a stellar cross section ratio of  $R_\sigma^* = 0.36 \pm 0.02$ . Using a simple exponential model for the chemical enrichment of  $^{187}\text{Re}$  over the galactic lifetime, we can estimate the impact of the capture cross section uncertainties on the nucleosynthesis time duration. This value turns out to be of the order of 0.5 Gyr. In other words, the uncertainty due to the nuclear physics input in the Re/Os clock can be presently estimated to be of the order of 0.5 Gyr.

Of course, for the age and for its complete uncertainty estimates, a full analysis with appropriate galactic chemical evolution modeling, as well as detailed calculation of the s-process abundances based on thermally pulsed AGB stars require a much more extended analysis which goes beyond the scope of the present contribution.

A full new coupled-channel calculation based on the results of the present analysis is underway and will be presented in further publications on the subject.

#### 5 Conclusions

A preliminary statistical analysis of the resolved resonance parameters for the  $^{186,187,188}\text{Os}$  neutron capture cross section measurements performed at CERN n\_TOF has been completed and the results reported here. Maxwellian average cross sections for the range of temperatures relevant for s-process nucleosynthesis have been derived from the combined information of the experimental data in the RRR and URR. The implications of this analysis for the s-process component of  $^{187}\text{Os}$  and the related estimation of the time-duration of the galactic nucleosynthesis through the Re/Os clock have been shortly outlined.

This work was partly supported by the European Commission under contract FIKW-CT-2000-00107.

#### References

1. D.D. Clayton, *ApJ* **139**, 637 (1964).
2. F. Bosch et al., *Phys. Rev. Lett.* **77**, 5190 (1996).
3. M. Mosconi et al. (these proceedings).
4. C. Borcea et al., *Nucl. Instrum. Meth. A* **513**, 523 (2003).
5. U. Abbondanno et al., The n\_TOF Collaboration, Report CERN-SL-2002-053 ECT (2003).
6. R. Plag et al., The n\_TOF Collaboration, *Nucl. Instrum. Meth. A* **496**, 425 (2003).
7. S. Marrone et al., *Nucl. Instrum. Meth. A* **517**, 389 (2004).
8. U. Abbondanno et al., The n\_TOF Collaboration, *Nucl. Instrum. Meth. A* **538**, 692 (2005).
9. F. Corvi et al., *Nucl. Sci. Eng.* **107**, 272 (1991); J.N. Wilson, et al. *Nucl. Instrum. Meth. A* **511**, 388 (2003).
10. U. Abbondanno et al., The n\_TOF Collaboration, *Nucl. Instrum. Meth. A* **521**, 454 (2004).
11. G. Aerts et al., Report DAPNIA-04-106, CEA/Saclay France, 2004.
12. N. Larson, Report ORNL/TM-9179/R7, Oak Ridge National Laboratory, 2006.
13. S.F. Mughabghab, *Atlas of Neutron Resonances* (Elsevier, 2006).
14. S.F. Mughabghab, *Neutron Cross Sections*, Vol. 1 (Academic Press, New York, 1981).
15. R.R. Winters et al., *Phys. Rev. C* **34**, 840 (1986).
16. M. Moore et al., *Phys. Rev. C* **18**, 1328 (1978).
17. M. Mosconi et al., The n\_TOF Collaboration, *Proceedings of Science*, PoS(NIC-IX)055.